

# Clinical Graph-Mediated Distillation for Unpaired MRI-to-CFI Hypertension Prediction

Dillan Imans<sup>1</sup>, Phuoc-Nguyen Bui<sup>2</sup>, Duc-Tai Le<sup>3</sup>, and Hyunseung Choo<sup>4</sup>

<sup>1</sup> Department of Computer Science and Engineering  
Sungkyunkwan University, Suwon, South Korea

<sup>2</sup> Research Convergence Institute  
Sungkyunkwan University, Suwon, South Korea

<sup>3</sup> Department of AI Systems Engineering  
Sungkyunkwan University, Suwon, South Korea

<sup>4</sup> Department of Electrical and Computer Engineering  
Sungkyunkwan University, Suwon, South Korea

**Abstract.** Retinal fundus imaging enables low-cost and scalable hypertension (HTN) screening, but HTN-related retinal cues are subtle, yielding high-variance predictions. Brain MRI provides stronger vascular and small-vessel-disease markers of HTN, yet it is expensive and rarely acquired alongside fundus images, resulting in modality-siloed datasets with disjoint MRI and fundus cohorts. We study this unpaired MRI–fundus regime and introduce Clinical Graph-Mediated Distillation (CGMD), a framework that transfers MRI-derived HTN knowledge to a fundus model without paired multimodal data. CGMD leverages shared structured biomarkers as a bridge by constructing a clinical similarity  $k$ NN graph spanning both cohorts. We train an MRI teacher, propagate its representations over the graph, and impute brain-informed representation targets for fundus patients. A fundus student is then trained with a joint objective combining HTN supervision, target distillation, and relational distillation. Experiments on our newly collected unpaired MRI–fundus–biomarker dataset show that CGMD consistently improves fundus-based HTN prediction over standard distillation and non-graph imputation baselines, with ablations confirming the importance of clinically grounded graph connectivity. Code is available at <https://github.com/DillanImans/CGMD-unpaired-distillation>.

**Keywords:** Hypertension · Cross-modal distillation · Biomarker graphs.

## 1 Introduction

Cardiovascular diseases remain a leading cause of global morbidity and mortality, underscoring the need for scalable methods to identify individuals at elevated vascular risk early [9]. Advances in computational imaging have enabled imaging-based risk phenotyping, where medical images are used to infer cardiometabolic and vascular risk factors at scale. High-fidelity modalities such as brain MRI can capture downstream injury patterns associated with chronic

vascular risk and small-vessel disease [4, 15]. However, MRI is costly and unevenly available, limiting population-scale deployment, particularly in resource-constrained settings [10, 7]. Retinal fundus imaging, by contrast, is inexpensive and widely deployable [11], but it provides an indirect and incomplete readout of vascular pathology. HTN-related retinal cues are often subtle, heterogeneous, and confounded, leading to weak and high-variance signals that challenge robust inference [13, 20, 17].

A natural strategy is to transfer high-fidelity vascular signal from brain MRI to scalable retinal fundus imaging via cross-modal knowledge distillation, treating MRI as the teacher and fundus as the student. However, most cross-modal distillation and representation-alignment methods implicitly assume paired multimodal data—i.e., both modalities are acquired for the same individual—so that the teacher can provide a sample-specific target (logits or features) for each student image. In practice, paired MRI–fundus acquisitions are rarely available at scale: fundus imaging is routine and inexpensive, whereas MRI is resource-intensive and typically ordered under different clinical indications. Consequently, obtaining both modalities often requires dedicated multimodality sub-studies rather than standard care pipelines [16]. This yields a disjoint multi-cohort regime in which the teacher modality is systematically missing for the student cohort, rendering conventional paired distillation inapplicable and limiting approaches that depend on a small paired subset. These constraints motivate methods that can establish cross-cohort correspondence without co-acquisition, for example by leveraging shared structured clinical variables as a linking signal.

Related work falls into three categories. First, paired cross-modal distillation [21] assumes paired acquisitions so a teacher on a superior modality can provide per-instance targets to supervise a student on a weaker modality. This assumption breaks when cohorts are disjoint and the superior modality is unavailable for the student cohort. Second, unpaired distillation [2, 8, 19] uses modality-bridging translation or reconstruction to transfer supervision without one-to-one pairing, e.g., CMEDL [8] for unpaired MRI→CT segmentation; these methods are largely tailored to closely related modalities of the same anatomy and do not address large modality gaps such as brain MRI→retinal fundus imaging. Third, EHR-based patient similarity learning [3] constructs clinical similarity graphs from structured variables, but has not been used to generate patient-specific distillation targets for cross-modal transfer across disjoint cohorts.

To this end, we propose the Clinical Graph-Mediated Distillation (CGMD), a framework that transfers vascular representations from brain MRI to scalable retinal fundus imaging without paired acquisitions. To the best of our knowledge, CGMD is the first distillation approach that supports cross-modal transfer across *disjoint cohorts* and *anatomically distinct* modalities (e.g., brain MRI→fundus) without subject-level correspondence. CGMD constructs a clinically grounded similarity graph from shared structured biomarkers, trains an MRI teacher on the MRI cohort, and propagates teacher embeddings over the graph to impute patient-specific distillation targets for fundus subjects in a separate cohort. A fundus student is then optimized with supervised HTN loss plus distillation to

the imputed targets, enabling MRI-free deployment at inference. In summary, our main contributions are three-fold:

- We formalize an unpaired, disjoint-cohort MRI–fundus transfer setting, where paired distillation is infeasible and synthesis-based alignment is ill-posed due to the large anatomical modality gap.
- We propose **Clinical Graph-Mediated Distillation** (CGMD) framework that uses shared structured biomarkers to build a clinical similarity graph and propagate MRI teacher embeddings, producing patient-specific distillation targets for fundus training without paired acquisition.
- On a newly collected unpaired MRI–fundus–biomarker dataset, CGMD consistently improves fundus-based HTN prediction over standard distillation and non-graph imputation baselines; ablations verify that clinically grounded graph connectivity is critical for effective cross-cohort transfer.

## 2 Methodology

Fig. 1 overviews our cross-cohort graph-mediated distillation pipeline for transferring MRI-derived knowledge to fundus without paired subjects. Given disjoint cohorts, an MRI set  $\mathcal{D}_B$  and a fundus set  $\mathcal{D}_F$ , we train an MRI teacher on  $\mathcal{D}_B$  and extract patient embeddings. Using shared clinical biomarkers, we construct a  $k$ NN graph over MRI patients and smooth the embeddings to obtain denoised teacher priors (Sec. 2.1). For each fundus patient in  $\mathcal{D}_F$ , we retrieve clinically nearest MRI patients and impute a patient-specific prior via weighted aggregation of the smoothed priors, using label-gating to encourage class-consistent transfer (Sec. 2.2). We then train a fundus student with supervised loss, distillation to the imputed priors, and a relational term aligning fundus embedding similarities with those imputed priors (Sec. 2.3). At inference, only fundus inputs and routine biomarkers are required; no MRI is needed.

### 2.1 MRI Teacher and Smoothed Priors

We first train an MRI teacher on  $\mathcal{D}_B$  and extract a teacher embedding  $z_i^{(0)} \in \mathbb{R}^d$  for each MRI patient  $i$ . If multiple MRI scans are available for a patient, we compute scan-level embeddings and average them to obtain  $z_i^{(0)}$ . Using the clinical biomarkers  $\{c_i^B\}$ , we construct a directed, weighted  $k$ -NN graph  $G_B$  by connecting each node  $i$  to its  $k$  nearest MRI neighbors  $\mathcal{N}_B(i)$  under cosine distance in biomarker space. Here,  $c_i^B \in \mathbb{R}^m$  is the patient’s preprocessed clinical biomarker feature vector (numeric features concatenated with one-hot categorical variables). For each directed edge  $(i \rightarrow j)$  with  $j \in \mathcal{N}_B(i)$ , we define the cosine distance  $d_{ij} = 1 - \cos(c_i^B, c_j^B)$ , convert it to a similarity weight  $w_{ij} = \exp(-d_{ij}^2/\sigma^2)$ , where  $\sigma > 0$  is a scale parameter controlling how quickly similarity decays with clinical distance, and normalize over  $\mathcal{N}_B(i)$ :

$$p_{ij} = \frac{w_{ij}}{\sum_{\ell \in \mathcal{N}_B(i)} w_{i\ell}}. \quad (1)$$

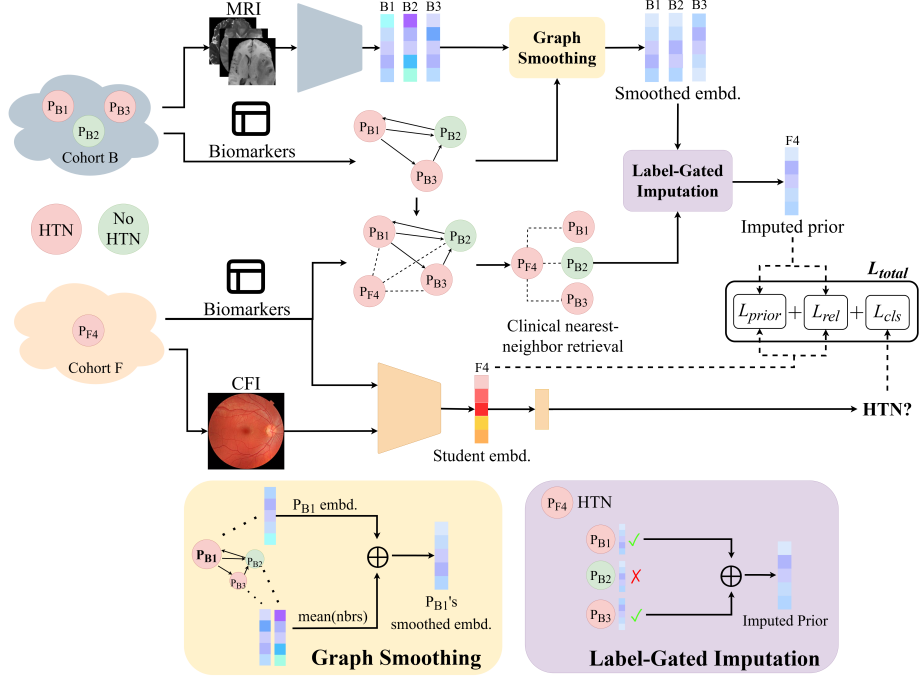


Fig. 1: Overview of the proposed CGMD. MRI teacher embeddings are smoothed on a clinical  $k$ NN graph to impute fundus priors, and the fundus student is trained with supervised, prior, and relational distillation (MRI-free inference).

We smooth teacher embeddings via one-step residual propagation:

$$\tilde{z}_i = \alpha z_i^{(0)} + (1 - \alpha) \sum_{j \in \mathcal{N}_B(i)} p_{ij} z_j^{(0)}, \quad (2)$$

where  $\alpha \in [0, 1]$  anchors the representation to the original teacher embedding. The smoothed embeddings  $\{\tilde{z}_i\}$  are used as teacher priors for cross-cohort imputation, denoising representations by aggregating information from clinically similar neighbors. This reduces variability from scan noise and individual outliers by borrowing signal from clinically similar patients.

## 2.2 Cross-cohort Prior Imputation

For each fundus patient  $u$ , we retrieve its top- $k$  clinically nearest MRI patients  $\mathcal{N}_B(u)$  by cosine distance between biomarkers ( $c_u^F, c_i^B$ ). Using the same distance-to-weight mapping and normalization as in Sec. 2.1, we obtain normalized neighbor weights  $\{p_{ui}\}_{i \in \mathcal{N}_B(u)}$  (defined analogously to  $p_{ij}$ ). To enforce class-consistent transfer, we apply label gating: for a fundus patient with label  $y_u^F$ , we restrict

retrieved neighbors to MRI patients with the same label,

$$\mathcal{N}_B^+(u) = \{i \in \mathcal{N}_B(u) : y_i^B = y_u^F\}. \quad (3)$$

We then renormalize  $p_{ui}$  over  $\mathcal{N}_B^+(u)$  so that  $\sum_{i \in \mathcal{N}_B^+(u)} p_{ui} = 1$ . If  $\mathcal{N}_B^+(u) = \emptyset$ , we fall back to the ungated neighborhood  $\mathcal{N}_B(u)$  (i.e., no label gating). The imputed teacher prior is computed as a weighted average of smoothed MRI priors,

$$\hat{z}_u = \sum_{i \in \mathcal{N}_B^+(u)} p_{ui} \tilde{z}_i. \quad (4)$$

Fundus data may contain multiple eye images per patient; for notational simplicity we treat each patient as having a single fundus sample. In practice, we compute  $\hat{z}_u$  once per patient and assign the same imputed prior to all images from the same patient during training. Intuitively, this yields a clinically matched teacher target for each fundus patient by borrowing representations from biomarker-similar MRI patients, enabling distillation across disjoint MRI–fundus cohorts.

### 2.3 Student training with prior and relational distillation

We train a fundus student on  $\mathcal{D}_F$  using supervised classification together with (i) distillation to imputed priors and (ii) a relational loss defined on a clinical similarity graph over the training fundus patients.

**Student model and classification loss.** Given a fundus input  $x_u^F$  for patient  $u$ , the student produces an embedding  $z_u \in \mathbb{R}^d$  which is  $\ell_2$ -normalized and concatenated with an MLP embedding of biomarkers  $h(c_u^F)$  before a single-logit prediction head. Let  $\ell_u \in \mathbb{R}$  denote the predicted logit for patient  $u$ . We supervise using binary cross-entropy on logits:

$$\mathcal{L}_{\text{cls}} = \frac{1}{|\mathcal{B}|} \sum_{u \in \mathcal{B}} \text{BCEWithLogits}(\ell_u, y_u^F), \quad (5)$$

where  $\mathcal{B}$  is a minibatch of fundus patients. This term trains the student to predict the label from fundus imaging (and biomarkers) under standard supervision.

**Prior distillation.** We match each fundus embedding to its patient-level imputed teacher prior using cosine distance. We  $\ell_2$ -normalize the imputed prior  $\hat{z}_u$  before computing cosine similarity:

$$\mathcal{L}_{\text{prior}} = \frac{1}{|\mathcal{B}|} \sum_{u \in \mathcal{B}} (1 - \cos(z_u, \hat{z}_u)). \quad (6)$$

This term transfers MRI-derived signal by aligning fundus embeddings to the imputed teacher prior for each patient.

**Fundus clinical graph and relational distillation.** To constrain relations

among student embeddings, we build a weighted clinical  $k$ -NN graph  $G_F = (V_F, E_F)$  over training fundus patients in biomarker space (cosine distance) and symmetrize it to obtain an undirected graph. We assign nonnegative edge weights  $\pi_{uv}$  using the same distance-to-weight mapping as in Sec. 2.1. Each patient  $u$  already has a label-gated imputed prior  $\hat{z}_u$  from Sec. 2.2; we  $\ell_2$ -normalize  $\hat{z}_u$  when computing cosine similarities and use these priors to define teacher-implied relations for relational matching. During training, we compute the relational loss only on train-graph edges whose endpoints co-occur in the current minibatch and we gate to same-label pairs ( $y_u^F = y_v^F$ ), yielding the within-batch edge set

$$\mathcal{E}_B = \{(u, v) \in E_F : u, v \in \mathcal{B}, y_u^F = y_v^F\}.$$

For each clinically similar pair  $(u, v) \in \mathcal{E}_B$  (with edge weight  $\pi_{uv}$ ), we match the student-space similarity to the teacher-implied similarity between their priors:

$$\mathcal{L}_{\text{rel}} = \frac{1}{\sum_{(u,v) \in \mathcal{E}_B} \pi_{uv}} \sum_{(u,v) \in \mathcal{E}_B} \pi_{uv} (\cos(z_u, z_v) - \cos(\hat{z}_u, \hat{z}_v))^2, \quad (7)$$

where  $\cos(\cdot, \cdot)$  denotes cosine similarity. If  $\mathcal{E}_B = \emptyset$ , we set  $\mathcal{L}_{\text{rel}} = 0$ . Intuitively, on clinical-neighbor pairs, we encourage student similarity  $\cos(z_u, z_v)$  to match teacher-implied similarity  $\cos(\hat{z}_u, \hat{z}_v)$ : similar priors pull embeddings together, while dissimilar priors push them apart. Same-label gating prevents imposing relational constraints across different disease states.

**Overall objective.** The training objective combines classification, prior distillation, and relational distillation:

$$\mathcal{L} = \lambda_{\text{cls}} \mathcal{L}_{\text{cls}} + \lambda_{\text{prior}} \mathcal{L}_{\text{prior}} + \lambda_{\text{rel}} \mathcal{L}_{\text{rel}}. \quad (8)$$

Here,  $\lambda_{\text{cls}}$ ,  $\lambda_{\text{prior}}$ , and  $\lambda_{\text{rel}}$  are scalar loss weights.

### 3 Experiments

**Dataset and Experimental Setup.** We study two private cohorts from a tertiary medical center: a brain MRI cohort (FLAIR;  $n=295$ ) and a retinal fundus cohort ( $n=112$ ). Cohorts are strictly disjoint at the patient level (no paired MRI–fundus subjects) and are linked only through 16 shared structured clinical variables (e.g., age, sex, and routine labs). The task is binary hypertension (HTN) prediction; SBP/DBP and explicit HTN diagnosis indicators are excluded to prevent label leakage. We use 5-fold patient-level stratified cross-validation, reporting patient-level AUC/AUPRC averaged across held-out folds. Operating-point metrics (sensitivity, specificity, F1) use the fold-specific threshold maximizing Youden’s  $J$  on the training split and then applied unchanged to the held-out validation split. For distillation baselines that require paired samples (KD [6], FitNets [14], RKD [12], SimKD [1]), we use label-consistent surrogate pairing: each fundus sample is matched (fixed seed) to 20 randomly sampled MRI patients with the same label, and supervision uses the mean teacher output across

Table 1: Patient-level comparison of distillation methods in the disjoint-cohort setting. The best results are highlighted in **bold**.

Method	AUC	AUPRC	Sensitivity	Specificity	F1
FDDM [18]	0.715±0.051	0.879±0.013	<b>0.815</b> ±0.179	0.679±0.182	0.709±0.032
SimKD [1]	0.732±0.134	0.869±0.075	0.705±0.234	0.786±0.192	0.761±0.155
RKD [12]	0.756±0.074	0.880±0.062	0.651±0.176	0.871±0.194	0.752±0.104
FitNets [14]	0.779±0.058	0.892±0.049	0.716±0.108	0.881±0.109	0.807±0.060
KD [6]	0.803±0.101	0.905±0.065	0.770±0.151	0.843±0.183	<b>0.832</b> ±0.084
<b>CGMD</b>	<b>0.855</b> ±0.127	<b>0.937</b> ±0.055	0.728±0.123	<b>0.933</b> ±0.149	0.826±0.087

matches; FDDM [18] follows its original protocol.

**Implementation Details.** Models are implemented in PyTorch (v2.2.2, CUDA 12.1) and trained on an NVIDIA RTX 2080 Ti. The MRI teacher uses a 2D ResNet-34 with multi-slice input (16 centered slices,  $256 \times 256$ ), while the fundus student uses a ResNet-18 on  $224 \times 224$  images with a clinical vector constructed from the 16 shared variables concatenated with pooled image features before the final classifier (except in biomarker-free ablations). We train for 50 epochs with learning rate  $1e-4$  and batch size 8 using standard preprocessing/augmentation such as horizontal flip and normalization. Clinical graphs are cosine k-NN ( $k=20$  for MRI;  $k=5$  for fundus). We set  $\lambda_{cls} = \lambda_{distill} = \lambda_{rel} = 1$ ,  $\sigma = 1$ , and  $\alpha = 0.9$ .

## 4 Performance evaluation

**Comparison with KD Methods.** Table 1 compares CGMD with distillation baselines adapted to our disjoint-cohort setting across AUC, AUPRC, sensitivity, specificity, and F1. Among the baselines, logit-based KD is strongest overall (AUC 0.803, AUPRC 0.905, F1 0.832), while FitNets and RKD are competitive but lower on AUC/AUPRC. CGMD yields the best ranking across the primary metrics, improving AUC by 0.052 and AUPRC by 0.032 over the best baseline, with the highest specificity (0.933) and comparable F1 (0.826). These gains indicate that clinically grounded graph-based imputation provides more informative teacher targets than label-matched surrogate pairing.

**Ablation Studies.** Table 2 breaks down the contribution of each CGMD component. Prior distillation alone provides a solid baseline, while adding MRI-graph smoothing yields a consistent AUC/AUPRC lift, supporting the hypothesis that smoothing denoises teacher embeddings before cross-cohort imputation. Using the relational loss without smoothing shifts the operating point toward higher sensitivity and F1 but with a drop in AUC. Combining distillation, smoothing, and relational matching achieves the best overall AUC/AUPRC and restores balanced performance, indicating that smoothing stabilizes the imputed targets so relational constraints become beneficial rather than over-regularizing. Over-

Table 2: Module ablation for CGMD using patient-level metrics. The best results are highlighted in **bold**.

Distill	Smooth	Rel	AUC	AUPRC	Sensitivity	Specificity	F1
✓	✗	✗	0.830±0.133	0.927±0.060	0.766±0.202	0.876±0.137	0.831±0.136
✓	✓	✗	0.844±0.120	0.925±0.066	0.714±0.158	<b>0.933</b> ±0.149	0.813±0.115
✓	✗	✓	0.815±0.116	0.907±0.064	<b>0.820</b> ±0.151	0.790±0.170	<b>0.853</b> ±0.090
✓	✓	✓	<b>0.855</b> ±0.127	<b>0.937</b> ±0.055	0.728±0.123	<b>0.933</b> ±0.149	0.826±0.087

all, the ablations suggest that clinical-graph smoothing is the key enabler that makes relational distillation effective in the disjoint-cohort regime.

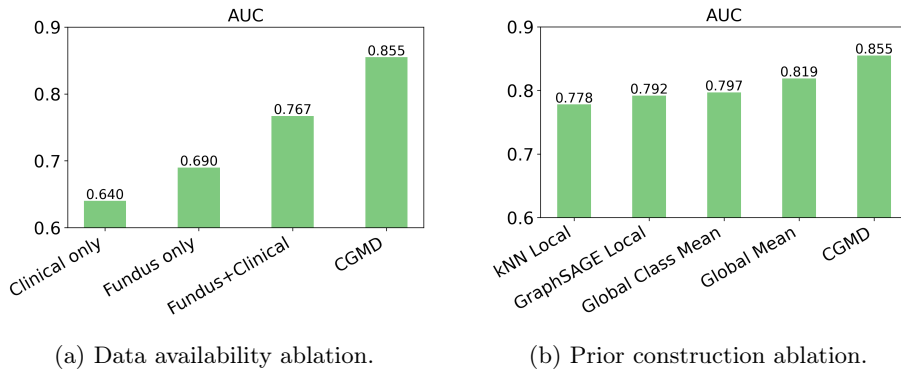


Fig. 2: Impact of (a) data availability and (b) prior construction strategies on the final HTN classification performance.

Fig. 2a ablates data availability: performance improves as more informative inputs are provided, and CGMD remains best overall, indicating that MRI→fundus transfer adds benefit beyond clinical features and/or fundus images alone (or simple concatenation). Fig. 2b ablates prior construction for the unpaired fundus cohort. Local baselines propagate teacher embeddings over a clinical similarity graph (kNN; GraphSAGE [5]) without label gating, while global baselines use class-conditional means (Global Class Mean) or cohort-level averages (Global Mean). CGMD outperforms all alternatives, supporting that combining patient-specific, graph-mediated priors with class-consistent (label-gated) aggregation is key for effective distillation in the disjoint-cohort setting.

## 5 Conclusion

We presented Clinical Graph-Mediated Distillation (CGMD) and formalized a practical new setting: disjoint-cohort cross-modal transfer, where modalities

come from separate cohorts and the teacher modality is missing for the student cohort. CGMD uses shared structured biomarkers to build a clinical similarity graph and propagate MRI teacher embeddings to generate patient-specific distillation targets for fundus training without paired acquisitions. On 5-fold patient-level cross-validation, CGMD outperformed adapted distillation baselines (AUC 0.855, AUPRC 0.937), and ablations confirmed the importance of clinically meaningful graph structure. Future work will extend CGMD to other disjoint-cohort modality pairs and clinical tasks.

**Disclosure of Interests.** The authors have no competing interests to declare that are relevant to the content of this article.

## References

1. Chen, D., Mei, J.P., Zhang, H., Wang, C., Feng, Y., Chen, C.: Knowledge distillation with the reused teacher classifier. In: Proceedings of the IEEE/CVF conference on computer vision and pattern recognition. pp. 11933–11942 (2022)
2. Dou, Q., Liu, Q., Heng, P.A., Glocker, B.: Unpaired multi-modal segmentation via knowledge distillation. *IEEE transactions on medical imaging* **39**(7), 2415–2425 (2020)
3. Gu, Y., Yang, X., Tian, L., Yang, H., Lv, J., Yang, C., Wang, J., Xi, J., Kong, G., Zhang, W.: Structure-aware siamese graph neural networks for encounter-level patient similarity learning. *Journal of Biomedical Informatics* **127**, 104027 (2022)
4. Hainsworth, A.H., Markus, H.S., Schneider, J.A.: Cerebral small vessel disease, hypertension, and vascular contributions to cognitive impairment and dementia. *Hypertension* **81**(1), 75–86 (2024)
5. Hamilton, W., Ying, Z., Leskovec, J.: Inductive representation learning on large graphs. *Advances in neural information processing systems* **30** (2017)
6. Hinton, G., Vinyals, O., Dean, J.: Distilling the knowledge in a neural network. arXiv preprint arXiv:1503.02531 (2015)
7. Hricak, H., Prior, J.O., Muellner, A., Abdel-Wahab, M., Allen, B., Atun, R., Cerri, G.G., Ngwa, W., Hierath, M., Scott, A.M.: Strengthening medical imaging capacity: the time is now. *The Lancet Oncology* **26**(1), 7–9 (2025)
8. Jiang, J., Rimner, A., Deasy, J.O., Veeraraghavan, H.: Unpaired cross-modality educed distillation (cmedl) for medical image segmentation. *IEEE transactions on medical imaging* **41**(5), 1057–1068 (2021)
9. Martin, S.S., Aday, A.W., Almarzooq, Z.I., Anderson, C.A., Arora, P., Avery, C.L., Baker-Smith, C.M., Barone Gibbs, B., Beaton, A.Z., Boehme, A.K., et al.: 2024 heart disease and stroke statistics: a report of us and global data from the american heart association. *Circulation* **149**(8), e347–e913 (2024)
10. Murali, S., Ding, H., Adedeji, F., Qin, C., Obungoloch, J., Asllani, I., Anazodo, U., Ntusi, N.A., Mammen, R., Niendorf, T., et al.: Bringing mri to low-and middle-income countries: directions, challenges and potential solutions. *NMR in Biomedicine* **37**(7), e4992 (2024)
11. Nakayama, L.F., Ribeiro, L.Z., Tabuse, C.L., Malerbi, F., Regatieri, C.: A comprehensive review of portable retinal cameras: Technical features, ai integration, and clinical potential. *AJO International* p. 100194 (2025)

12. Park, W., Kim, D., Lu, Y., Cho, M.: Relational knowledge distillation. In: Proceedings of the IEEE/CVF conference on computer vision and pattern recognition. pp. 3967–3976 (2019)
13. Poplin, R., Varadarajan, A.V., Blumer, K., Liu, Y., McConnell, M.V., Corrado, G.S., Peng, L., Webster, D.R.: Prediction of cardiovascular risk factors from retinal fundus photographs via deep learning. *Nature biomedical engineering* **2**(3), 158–164 (2018)
14. Romero, A., Ballas, N., Kahou, S.E., Chassang, A., Gatta, C., Bengio, Y.: Fitnets: hints for thin deep nets (2014). arXiv preprint arXiv:1412.6550 **3** (2014)
15. Sole-Guardia, G., Custers, E., de Lange, A., Clijckne, E., Geenen, B., Gutierrez, J., Kusters, B., Claassen, J., de Leeuw, F.E., Wiesmann, M., et al.: The impact of chronic hypertension on small vessel disease–neuroinflammation beyond white matter hyperintensities. *Cerebral Circulation-Cognition and Behavior* **6**, 100313 (2024)
16. Sun, J., Hui, Y., Li, J., Zhao, X., Chen, Q., Li, X., Wu, N., Xu, M., Liu, W., Li, R., et al.: Protocol for multi-modality medical imaging study based on kailuan study (meta-cls): rationale, design and database building. *BMJ open* **13**(2), e067283 (2023)
17. Tan, W., Yao, X., Le, T.T., Tan, B., Schmetterer, L., Chua, J.: The new era of retinal imaging in hypertensive patients. *The Asia-Pacific Journal of Ophthalmology* **11**(2), 149–159 (2022)
18. Wang, L., Dai, W., Jin, M., Ou, C., Li, X.: Fundus-enhanced disease-aware distillation model for retinal disease classification from oct images. In: International Conference on Medical Image Computing and Computer-Assisted Intervention. pp. 639–648. Springer (2023)
19. Yang, F., Li, X., Wang, B., Teng, P., Liu, G.: Umscs: a novel unpaired multimodal image segmentation method via cross-modality generative and semi-supervised learning. *International Journal of Computer Vision* **133**(7), 4442–4464 (2025)
20. Zhang, L., Yuan, M., An, Z., Zhao, X., Wu, H., Li, H., Wang, Y., Sun, B., Li, H., Ding, S., et al.: Prediction of hypertension, hyperglycemia and dyslipidemia from retinal fundus photographs via deep learning: A cross-sectional study of chronic diseases in central china. *PloS one* **15**(5), e0233166 (2020)
21. Zhao, L., Peng, X., Chen, Y., Kapadia, M., Metaxas, D.N.: Knowledge as priors: Cross-modal knowledge generalization for datasets without superior knowledge. In: Proceedings of the IEEE/CVF Conference on Computer Vision and Pattern Recognition. pp. 6528–6537 (2020)